Ni-Bisdipyrrin Metalloligand as Potential Sensitizer in MOFs: Synthesis and Photoelectrochemical Characterization

Alessandro Poma,[a] Ivan Grigioni,[a] Maria Vittoria Dozzi,[a] Stéphane Baudron,[b] Lucia Carlucci,[a] Mir Wais Hosseini,[b] Elena Selli[a,*]

[a] Dipartimento di Chimica, Università degli Studi di Milano, Via Golgi 19, I 20133 Milano, Italy

[b] Laboratoire de Tectonique Moléculaire, UMR CNRS 7140, icFRC, Université de Strasbourg, F-67000, Strasbourg

Abstract

A Ni-based 2,2'-bisdipyrrin molecule bearing peripheral benzoic acid groups (Ni-bisdpmCOOH) have been synthesized and characterized. Electrochemical tests evidence a high LUMO energy on the molecule that, combined with its absorption properties extending up to the NIR region, may allow sensitization of thermodynamically uphill reactions, such as proton and carbon dioxide photoreduction. Therefore, a sensitized photo-anode was prepared by adsorbing Ni-bisdpmCOOH onto a TiO_2 film, which showed an incident photon to current efficiency, measured at 0.61 V vs RHE, extending to visible light region. Thus, the photo-electronically excited Ni-bisdpmCOOH is effectively able to inject electrons into the conduction band of TiO_2. Moreover, the Ni-bisdpmCOOH complex was successfully incorporated into the Zr-containing UiO-66 metal organic framework (MOF) through the one-pot mixed-ligands approach, thus obtaining a material that combines the visible light activity of Ni-bisdpmCOOH with the high chemical stability of UiO-66.

1. Introduction

While the most studied class of dyes based on the dipyrrin backbone is the boron-dipyrromethene (BODIPY) characterized by high chemical and photochemical stability,[1] several examples of luminescent metal-dipyrrin based complexes have also been reported.[2] Dipyrrin complexes containing Rh(III),[3] Cu(I),[4] Pt(II),[5] Ir(III) [6] and Zn(II) [7] are already known. Among these the Zn(II) derivatives are more widely investigated and in such systems was shown that the steric hindrance of the peripheral aryl group affect the fluorescence quantum yield and the excited state lifetime.[7b]

2,2'-Bis-dipyrrins comprising two dipyrrin fragments connected by a single C-C bond can be regarded as open chain version of corroles.[8] Even though this class of molecules has been described long ago,[9] their use has been mostly limited to the preparation of ~~the~~ helicate complexes.[10] Moreover, although these systems may show promising photophysical and electrochemical properties, a systematic and detailed investigation of such features is still lacking and only few reports in this field have been published so far.[10c,11]

In this work we synthesized a Ni-based 2,2'-bisdipyrrin complex (Ni-bisdpmCOOH) with absorption properties extending up to the NIR region of the spectrum. The photophysical and electrochemical characterization of this molecule evidenced a suitable position of its LUMO energy level with respect to the H^+/H_2 redox couple. Furthermore, with the aim to develop a photoactive heterogeneous material we incorporated the Ni-bisdpmCOOH unit into a robust metal organic framework (MOF) architecture. Indeed, although dipyrrin complexes have been used as linkers in MOF structures,[12] this is the first example of bisdipyrrin-based metalloligand implemented into a Zr-based MOF.

2. Experimental section

2.1. Reagents and synthesis

All commercial chemicals were used as received from suppliers (Sigma-Aldrich, TCI Europe and Fluorochem) without further purification. Solvents were dried prior use. Complexes ***Ni-dpmCOOMe***, ***Ni-bisdpmCOOMe*** (see Scheme 1) and demetalated ***bisdpmCOOH*** were prepared according to reported procedures.[13,10c]

Synthesis of ***Ni-bisdpmCOOH***. ***Ni-bisdpmCOOMe*** (100.0 mg, 0.164 mmol) was dissolved in a mixture of THF, NaOH 1.0 M and H_2O (3/1/1, 25 mL total volume) and refluxed overnight. After cooling the mixture to room temperature (RT), the organic solvent was removed under reduced pressure and the water phase was acidified by addition of 1.0 M HCl solution until pH of 6.5 with the consequent precipitation of ***Ni-bisdpmCOOH*** as black powder. It was thus recovered by filtration, washed with water and finally dried in air (69.6 mg, 72.5%). ^{1}H NMR (300 MHz, DMSO-d_6) δ: 8.09 (d, J = 8.1 Hz, 5H[14]), 7.69 (d, J = 8.1 Hz, 5H), 6.83 (d, J = 4.2 Hz, 2H), 6.74 (d, J = 4.4 Hz, 2H), 6.71 (d, J = 4.2 Hz, 2H), 6.56 (d, J = 4.2 Hz, 2H), 6.02 (s, 2H). ESI-MS: *m/z* = 581.37 [M – H$^+$].

Synthesis of **UiO-66 MOF**. $ZrCl_4$ (30 mg, 0.129 mmol), 1,4-benzenedicarboxylic acid (BDC, 30 mg, 0.180 mmol) and benzoic acid (500 mg, 4.094 mmol) were added to 3 mL of DMF and dissolved by ultrasonication in a Pyrex vial. The mixture was heated in an oven at 85 °C for 24 h. The suspension was cooled to RT and the white powder was recovered by centrifugation. The solid was firstly washed with DMF for three times to remove unreacted precursors, and then treated for three times with acetone for the solvent-exchange. The resulting **UiO-66 MOF** white powder was thus recovered by centrifugation, and finally dried in an oven at 80 °C.

Synthesis of ***Ni-bisdpmCOOH@UiO-66 MOF***. $ZrCl_4$ (30 mg, 0.129 mmol), 1,4-benzene-dicarboxylate (BDC, 20 mg, 0.120 mmol), Ni-bisdpmCOOH complex (5 mg, 0.0086 mmol) and benzoic acid (600 mg, 4.918 mmol) were added to 2 mL of DMF and dissolved by ultrasonication in a Pyrex vial. The mixture was heated in an oven at 120 °C

for 12 h. By cooling down to RT, the precipitate characterized by a shiny black colour was collected by centrifugation. The solid was thus washed with DMF three times to remove unreacted precursors, and then solvent-exchanged with acetone for three times. The resulting ***Ni-bisdpmCOOH@UiO-66 MOF*** black powder was obtained by centrifugation, and dried in an oven at 80 °C.

Synthesis of [5,10,15,20-Tetrakis(4-carboxyphenyl)porphyrinato]-Ni(II) (**NiTCPP**).

Step 1: synthesis of [5,10,15,20-Tetrakis(4-methoxycarboxyphenyl)porphyrin] **(TCPPCOOMe)**. In a 500 mL 3-necked flask pyrrole (3.0 mL, 0.043 mol), methyl 4-formylbenzoate (6.9 g, 0.042 mol) were added to propionic acid (100 mL) and the solution was thus refluxed overnight in the darkness. After cooling to RT, the precipitation of **TCPPCOOMe** as microcrystalline dark powder occurred. This solid was collected by vacuum filtration, firstly washed with propionic acid and then with water and finally dried in an oven at 80 °C. Yield = 2.5 g (17.5%). ^{1}H NMR (300 MHz, $CDCl_3$) δ: 8.82 (s, 8H), 8.45 (d, J = 8.3 Hz, 8H), 8.29 (d, J = 8.25 Hz, 8H), 4.11 (s, 12H), -2.81 (bs, 2H).

Step 2: synthesis of [5,10,15,20-Tetrakis(4-methoxycarbonylphenyl)porphyrinato]-Ni(II) **(NiTCPPCOOMe)**. A solution of TPPCOOMe (500.0 mg, 0.59 mmol) and $NiCl_2{\cdot}6H_2O$ (1.80 g, 7.57 mmol) in 60 mL of DMF was refluxed for *ca.* 5 h. After cooling to RT, the addition of *ca.* 150 mL of water induced the precipitation of **NiTCPPCOOMe** as dark powder. The solid was filtered, and subsequently washed with water and 1 M HCl until the filtrate was colourless. The obtained crystalline powder (in quantitative yield) was dried in an oven at 80 °C and directly used in the following step without further purification.

Step 3: synthesis of [5,10,15,20-Tetrakis(4-carboxyphenyl)porphyrinato]-Ni(II) **(NiTCPP)**. NiTPPCOOMe (500 mg) was stirred in a mixture of THF and MeOH (25 mL each), to which a solution of NaOH (2.4 g, 60 mmol) in water (25 mL) was added. This mixture was refluxed overnight. After cooling to RT, THF and MeOH were removed under vacuum and the volume was restored by addition of water. The mixture was refluxed for

ca. 30 min in order to obtain a homogeneous solution, which was acidified with 1 M HCl until no further precipitate was detected. The solid was then filtered, washed with water until filtrate was colourless and dried in an oven at 80 °C.

2.2. Photoelectrodes preparation

The photoanodes were prepared by firstly depositing a commercial TiO_2 paste (Ti-Nanoxide T/SP, Solaronix) on a fluorine tin oxide (FTO) electrode through the so called *doctor-blade* technique, followed by the adsorption of Ni-bisdpmCOOH through electrostatic interactions between the carboxylic groups of the Ni complex and the -OH units on TiO_2 surface. In detail, the FTO electrode was covered with a scotch tape (3M), thus obtaining a 0.25 cm^2 exposed surface. A small amount of the TiO_2 paste was spread onto the surface with the aid of a microscope slide. Then, the scotch tape was removed and the electrodes were kept at 70 °C for 1 h and finally annealed at 500 °C for 1 h. The so-obtained TiO_2 – covered FTO electrodes were covered by few drops of a solution of Ni-bisdpmCOOH in DMF (concentration *ca.* 10^{-3} M) and left to dry in air. The not adsorbed dye was removed by washing with DMF and the absorption spectrum of the clean electrode was recorded. This procedure was repeated until no further increase in absorbance was detected. A total of 10 cycles were performed to reach the final absorbance value.

The TiO_2 – covered FTO modified with NiTCPP was obtained in the same way, by using a 0.5 mM solution of NiTCPP in DMF.

2.3. Structural and Photo(electro)chemical Characterization

Nuclear Magnetic Resonance (NMR) data were collected on a Bruker AVANCE 400 (400 MHz) at room temperature. The chemical shifts and coupling constants values are given in ppm and Hz, respectively.

ESI-MS analyses were performed by using a LCQ Fleet ion trap mass spectrometer with an electrospray ionisation source and an 'Ion Trap' mass analyser. The sample was solubilized in methanol and traces of DMF were added in order to promote the solubility of the compound. The MS spectra were obtained by direct infusion of the sample's solution under ionisation, ESI negative mode. Full-scan mass spectra were recorded in the mass/charge (*m/z*) range of 50–2000.

UV-Vis-NIR studies were performed with a Perkin-Elmer Lambda 650 S spectrometer with a resolution of 2 nm and a mean sampling rate of 200 nm/min. UV-Vis-NIR reflectance studies were performed with a Perkin–Elmer Lambda 950 spectrometer (spectra recorded in the reflection mode, using a 150 mm integrating sphere) with a resolution of 2 nm and a mean sampling rate of 200 nm/min.

Cyclic voltammetry was performed in a conventional three-electrode cell using an Autolab PGSTAT 12 (EcoChemie, Utrecht, The Netherlands). The potentiostat was controlled by NOVA software (version 2.1). The working electrode was a glassy carbon (GC) electrode with a 0.071 cm^2 surface area, a Pt wire was the counter electrode, with Ag/AgCl as reference electrode.

The ferrocene ($Fc^+|Fc$) electrode was used as reference after every measurement. For instance, the observed peak potential (E_p) of the molecule can be expressed with respect to the Fc+|Fc redox couple by simply subtracting to Ep the $Fc^+|Fc$ half-height peak value, calculated as $E_{p/2(Fc+|Fc)} = (E_{p,a(Fc+|Fc)} + E_{p,c(Fc+|Fc)}) / 2$, with $E_{p,a}$ and $E_{p,c}$ referring to the anodic and cathodic peaks, respectively. Moreover E_p values can be converted into the NHE scale by using the following equation: $E_{NHE} = (E_p - E_{p/2(Fc+|Fc)}) + E°_{Fc+|Fc} - E°_{H+/H_2}$, with $E°_{Fc+|Fc}$ corresponding to the potential value of $Fc^+|Fc$ couple referred to vacuum (equal to 4.8 V) and with $E°_{H+/H_2}$ referring to the potential value of H^+/H_2 couple referred to vacuum (equal to 4.44 V).

Photoelectrochemical measurements were performed using a home-made 3-arms cell and the same potentiostat employed for cyclic voltammetry analysis, with the photoelectrode as working electrode (0.25 cm^2 active surface), a Pt gauze as counter electrode and an Ag/AgCl (3 M NaCl) as reference electrode. The photoelectrodes were tested under back side illumination (through the FTO/TiO_2/***Ni-bisdpmCOOH*** interface). The light source was an Oriel, Model 81172 Solar Simulator with different cut-off filters (420 and 550 nm). The power intensity of the unfiltered AM 1.5G light, measured by means of a Thorlabs PM200 power meter equipped with a S130VC power head with Si detector, was 100 W cm^{-2}. A 0.5 M Na_2SO_3 aqueous solution buffered at pH = 7 with potassium phosphate was used in photoelectrochemical measurements. The potential vs. Ag/AgCl was converted into the RHE scale using the following equation: $E_{RHE} = E_{Ag/AgCl} + 0.059\ pH + E°_{Ag/AgCl}$, with $E°_{Ag/AgCl\ (3.0\ M\ NaCl)} = 0.210$ V at 25°C.

Incident photon-to-current efficiency (IPCE) measurements were carried out using a 300 W Lot-Oriel Xe lamp equipped with a Lot-Oriel Omni-λ 150 monochromator and a Thorlabs SC10 automatic shutter. A 0.62 V bias vs RHE was applied and the current was measured with a 20 nm step, within the 400 to 900 nm wavelength range. The incident light power was measured at each wavelength using the above mentioned calibrated Thorlabs photodiode and power meter. The IPCE was calculated at each wavelength by using the following equation:

$$IPCE = \frac{[1240 \cdot j]}{P_\lambda \cdot \lambda} \cdot 100$$

where j is the photocurrent density (mA cm^{-2}) and P_λ (nW cm^{-2}) is the power of the monochromatic light at wavelength λ (nm).

The internal quantum efficiency (IQE) was calculated by combining the IPCE spectrum with the absorption (A) spectrum of the photoanode:

$$IQE = \frac{IPCE}{1 - 10^{-A}}$$

X-ray powder diffraction (XRPD) was measured with a BRUKER D8-Focus Bragg-Brentano X-ray Powder Diffractometer equipped with a Cu sealed tube (λ = 1.54178) at 40 kV and 40 mA.

3. Results and discussion

3.1. Synthesis of Ni-bisdpmCOOH

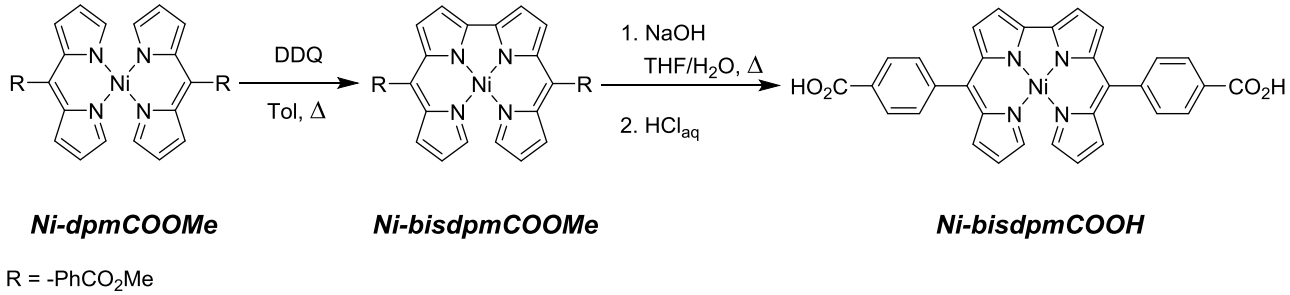

Ni-dpmCOOMe ***Ni-bisdpmCOOMe*** ***Ni-bisdpmCOOH***

Scheme 1 *– Synthesis of the 2,2'-bisdipyrrin Ni(II) metalloligand*

The synthetic route to ***Ni-bisdpmCOOH*** complex is depicted in Scheme 1. The saponification of ***Ni-bisdpmCOOMe*** complex was carried out as described by Brückner *et. al.*,[15] with a modification for the acidification step, which was carried out up to pH value of *ca.* 6. Because of the poor solubility of the ***Ni-bisdpmCOOH*** complex, the ^{13}C NMR spectrum could not be recorded. The successful saponification of the ester groups was confirmed by the absence of the methyl group signals in the upfield region of the ^{1}H NMR spectrum of complex ***Ni-bisdpmCOOH*** (See Fig. S1). On the other hand, the evidence of the retention of the Ni in the coordinating environment of the molecule is confirmed by the mass spectra analysis, which shows a peak of *m/z* value of 581.37, corresponding to the $[M - H^+]$ structure.

3.2. Optical Properties

The absorption spectrum of ***Ni-bisdpmCOOH***, recorded in DMF (concentration of $2.92 \cdot 10^{-5}$ M) is shown in Fig. 1, in comparison with the spectra of ***Ni-dpmCOOMe*** and ***Ni-bisdpmCOOMe*** complexes. ***Ni-bisdpmCOOH*** displays the maximum absorption peak at 416 nm, accompanied by less intense and broader peaks at 563, 770 and 846 nm. This absorption spectrum is similar to those previously reported for 2,2'-bisdipyrrin molecules[10b,c,11] and fully comparable with that of ***Ni-bisdpmCOOMe*** complex. On the contrary, ***Ni-dpmCOOMe*** shows an absorption edge at 570 nm with a unique strong absorption band at 464 nm and shoulders at *ca.* 440 and 500 nm.

The different absorption properties of ***Ni-bisdpmCOOH*** and ***Ni-bisdpmCOOMe*** complexes with respect to ***Ni-dpmCOOMe*** can be attributed to the increased conjugation and molecular rigidity ensured by the 2,2'-pyrrolic C-C bond. This difference is also evidenced by a comparison between the Ni coordination geometry in the two crystal structures. In fact, while ***Ni-dpmCOOMe*** shows a distorted tetrahedral geometry with an angle between the two bipyrrolic moieties of ca. 56° in ***Ni-bisdpmCOOMe*** the same angle decreses to *ca*. 23°, thus indicating a distorted square planar geometry.[10c]

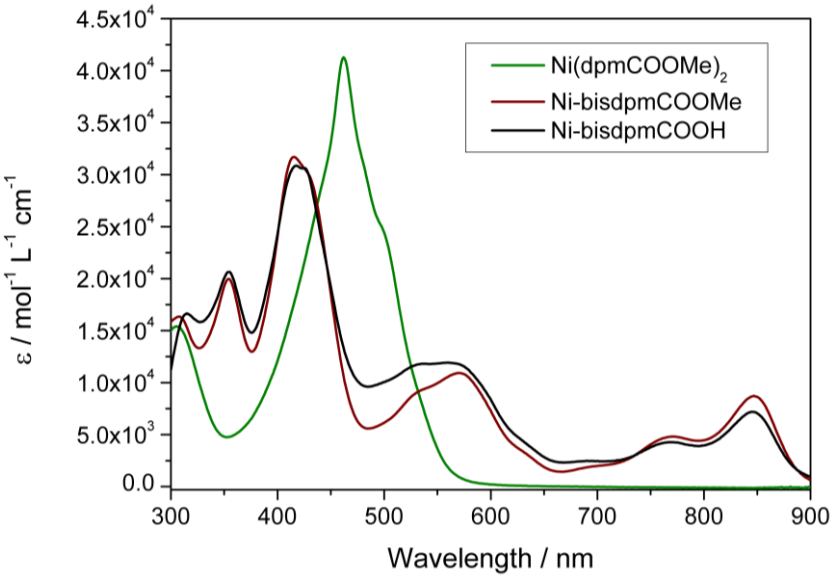

Figure 1 *– Comparison between absorption spectrum of* ***Ni-dpmCOOMe***, ***Ni-bisdpmCOOMe*** *and* ***Ni-bisdpmCOOH*** *in DMF.*

3.3. Electrochemical Characterization

The redox properties of the ***Ni-bisdpmCOOH*** complex were determined by cyclic voltammetry measurements in a DMF solution ($3 \cdot 10^{-4}$ M) containing 0.1 M tetra-*N*-butylammonium hexafluorophosphate ($TBAPF_6$) as supporting electrolyte under an inert atmosphere, attained by bubbling N_2 in the solution for 10 min. The cyclic voltammetry curves obtained at different potential scanning rate are compared in Fig. 2.

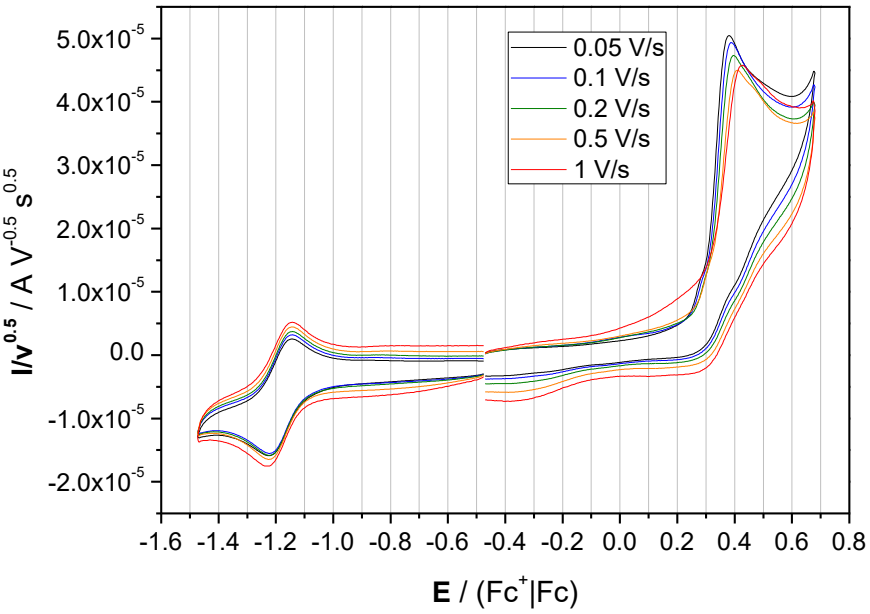

Figure 2 *– Anodic (positive potentials) and cathodic (negative potentials) scans of* ***Ni-bisdpmCOOH*** *complex around the first redox potentials performed at different potential scanning rates.*

The shape of the curve in the anodic part (positive potentials) evidences an irreversible bi-electronic oxidation process at 0.382 V *vs.* $Fc^+|Fc$ for the Ni-bisdipyrrin metalloligand. Moreover, the shift of the anodic oxidation potential position with the scan rate implies an electrochemically irreversible electron transfer. Differently, in the cathodic region (negative potentials), the complex displays a chemically and electrochemically reversible one-electron reduction at -1.21 V *vs.* $Fc^+|Fc$. These electrochemical processes are assigned to ligand-centred electron transfer processes[10a] by analogy with the redox properties already found for other similar Ni-bisdipyrrin complexes. In particular, with

respect to the molecule investigated by Bröring et. al.,[10b] *i.e.* containing fully alkylated pyrrolic fragments of the substituted Ni bisdipyrrin complex, ***Ni-bisdpmCOOH*** metalloligand displays a significant shift of both cathodic and anodic peaks towards more positive potentials. This effect can be due to a relative electron depletion induced by the absence of alkyl groups on the bisdipyrrin core[10b], which commonly behave as electron-donating groups.

By considering the first oxidation and reduction peaks reported in Fig. 2, the HOMO and the LUMO energy levels of ***Ni-bisdpmCOOH*** complex were located at 0.74 and -0.85 V *vs.* NHE, respectively, with a HOMO-LUMO gap value corresponding to 1.59 eV, which is slightly lower with respect to the 1.62 eV calculated for the fully alkylated dipyrrin molecules studied by Bröring et. al.[10b]

This difference can be again ascribed to the alkyl chains, that in the bisdipyrrin complex reported by Bröring et. al.[10b] make the molecule more electron rich but less planar and conjugated.

On the other hand, the presence of electron attracting carboxyl substituents on the phenyl ring of ***Ni-bisdpmCOOH*** should not affect the electronic properties, since the phenyl groups are twisted with respect to the bisdipyrrin core.[10c]

For the sake of comparison, the cyclic voltammetry of nickel tetracarboxyphenyl porphyrin (NiTCPP) displays, in the anodic part, a chemically reversible (at high scan rates) and electrochemically irreversible oxidation peak at 0.66 V *vs.* $Fc^+|Fc$. In the cathodic part, the NiTCPP shows a chemically reversible and electrochemically quasi-reversible reduction peak at -1.60 V *vs.* $Fc^+|Fc$ (see Fig. S3). The HOMO and LUMO energy levels are found at 1.03 and -1.24 V *vs* NHE, respectively (Fig. 3).

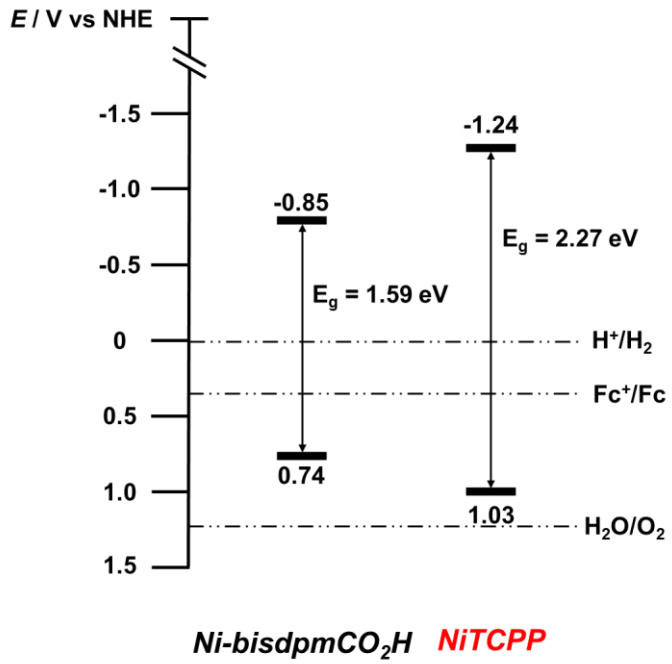

Figure 3 *– HOMO and LUMO energy levels of* ***Ni-bisdpmCOOH*** *and NiTCPP .*

Interestingly, the LUMO position of both ***Ni-bisdpmCOOH*** and NiTCPP are higher in energy with respect to both the TiO_2 conduction band (CB) position (*i.e.* -0.16 V vs NHE)[16] and the H^+/H_2 reduction potential.[17] Therefore, according to the relative energy level positions reported in Fig. 3, the electron injection from the LUMO of both the photoexcited complexes towards TiO_2 CB is allowed, making these systems potentially able to reduce protons from water into hydrogen under visible light irradiation.

3.4. Photoelectrochemical Characterization

The Uv-Vis-NIR absorption spectra of TiO_2-covered electrodes modified by subsequent deposition of ***Ni-bisdpmCOOH*** molecules are reported in Fig. 4. In particular, each absorption profile is given as the difference between the spectrum of the electrode containing the adsorbed dye and that prepared by depositing the only bare TiO_2 paste.

By comparing these spectra with that reported in Figure 1, a similar absorption profile of the dye adsorbed onto the TiO_2 paste with that of the free molecule in solution can be observed, apart from a slight blue-shift of the main peak with a maximum at 416 nm. This

could be a consequence of the subtracting procedure of the bare TiO_2 paste spectrum, characterized by a residual absorption tail up to 450 nm (Fig. S4).

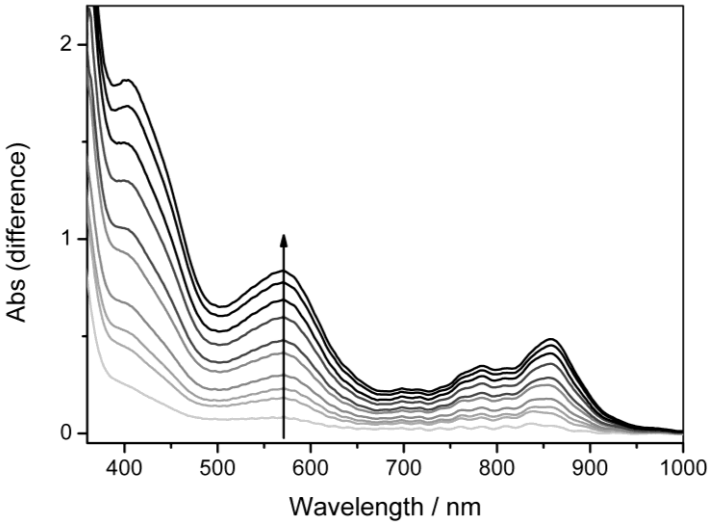

Figure 4 *– UV-vis absorption spectra indicating the progressive increase of adsorbed* ***Ni-bisdpmCOOH*** *on the TiO_2-covered electrodes. Each profile is obtained by subtracting the bare TiO_2 paste spectrum.*

The photoelectrochemical (PEC) performances of the modified electrode were explored by means of different photoelectrochemical analyses. Figure 5a shows the linear sweep voltammetry (LSV) curves of ***Ni-bisdpmCOOH*** on TiO_2 in the 0.22 to 0.62 V *vs.* RHE potential range. The curves clearly show the presence of photocurrent upon illumination with simulated solar irradiation along with 420 nm filter. The chronoamperometric curves recorded at 0.62 V vs RHE shown in Figure 5b clearly indicate the presence of photocurrent for the photoanode sensitized by ***Ni-bisdpmCOOH*** also with the 550 nm filter, while no photocurrent was detected with a bare TiO_2 electrode even with the 420 nm filter. Also when reference NiTCPP was employed as sensitizer on the TiO_2 electrode a negligible photocurrent response was detected with the 420 nm cut-off filter (see Fig. 5b), although this molecule shows an absorption tail in this spectral region, due to the intense Soret band and the single Q band centred at 532 nm (see Fig. S5). The low photocurrent response for NiTCPP molecule can be due to different variables

affecting the electron transfer (ET) rates, such as the molecular structure and the adsorption conditions, which have a large impact on molecular packing, geometry and aggregation of the porphyrin molecule onto the TiO_2 paste, eventually affecting the photocurrent response.[18]

The IPCE curve shown in Fig. 5c clearly demonstrates that ***Ni-bisdpmCOOH*** adsorbed on TiO_2 is a rather good sensitizer and that electron injection from photoexcited ***Ni-bisdpmCOOH*** to the TiO_2 conduction band may occur up to 620 nm. Moreover, the IQE curve is similar to the IPCE curve, due to the relatively high absorbance of ***Ni-bisdpmCOOH*** in the prepared photoanodes (see Fig. 4).

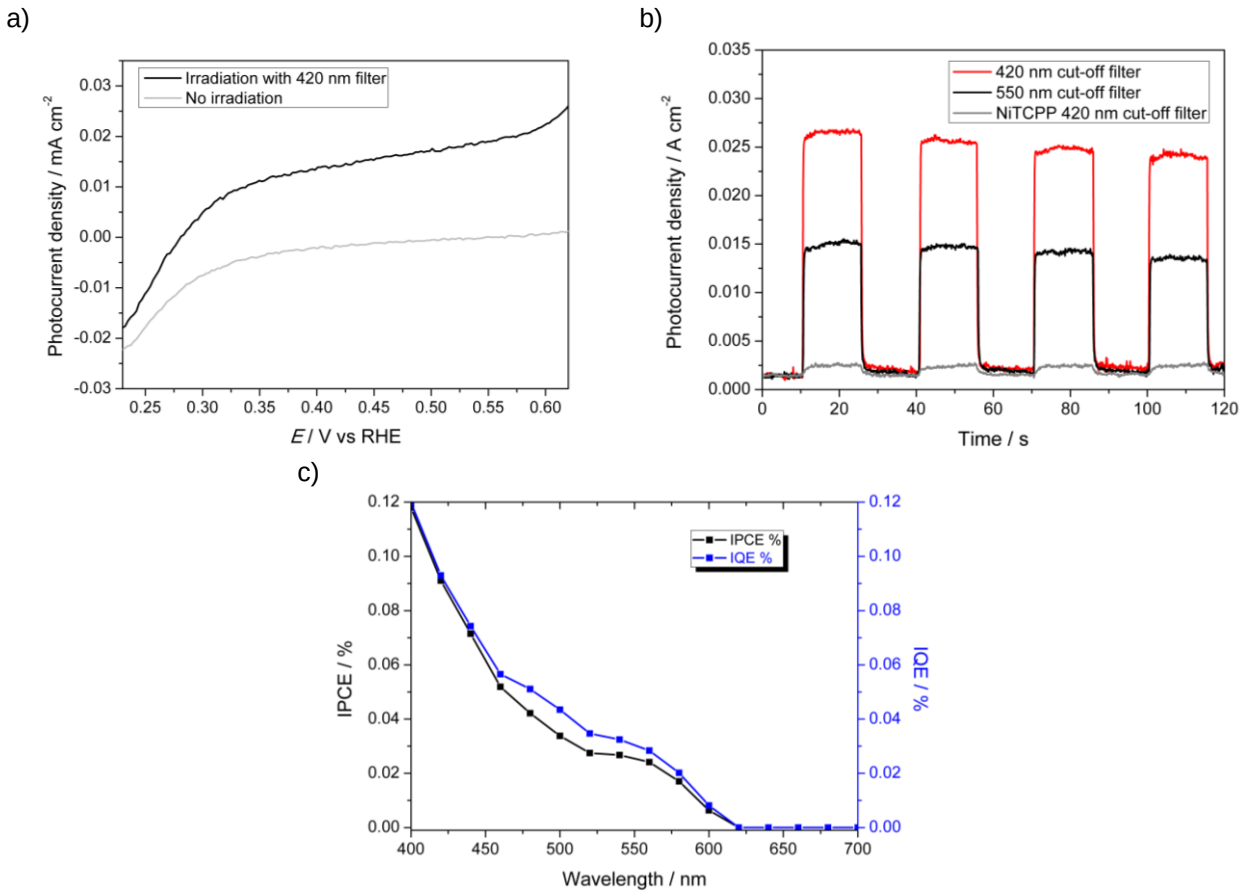

Figure 5 *– (a) Linear sweep voltammetry curves of* ***Ni-bisdpmCOOH****/TiO_2 under irradiation and in the dark, (b) Chronoamperometric analysis of the* ***Ni-bisdpmCOOH****/TiO_2 anode with different cut-off filters (thick lines) and of a TiO_2-based photoanode sensitized with reference NiTCPP with the 420 nm cut-off filter; (c) IPCE and IQE curves obtained with the* ***Ni-bisdpmCOOH****/TiO_2 electrode.*

3.5. Inclusion of *Ni-bisdpmCOOH* into the UiO-66 Framework

The integration of multi-functionalities into MOF structures has a great importance to extend the use of these meterials to a wide range of applications. Starting from the pioneering studies by Yaghi and co-workers.[19], the mixed-ligand approach still represents the most used method for the synthesis of multifunctional MOFs, which is based on the partial substitution of the main linker with a different (auxiliary) linker, with the preservation of the overall MOF structure.

Of course this implies that the auxiliary linker needs to possess the same geometry and coordinating ability of the "main linker" to make them "indistinguishable" during the self-assembling process, thus preventing the undesired formation of mixed phases.

Among the great variety of known MOF structures it is well known that Zr(IV)-based frameworks show the best chemical stability in a wide range of conditions (temperature, pH, solvents, etc) making them very interesting for many applications.

In the present work we pursued the idea to fruitfully exploit the visible light absorption and electron injection abilities of ***Ni-bisdpmCOOH*** complex by its integration as auxiliary linker into a robust Zr-based MOF structure. We thus chose UiO-66 MOF, because apart from its high chemical stability and synthetic reproducibility, it is characterized by a conduction band potential which is less negative with respect to the LUMO level of ***Ni-bisdpmCOOH,*** i.e. being located at -0.60 V [20] and -0.85 V vs NHE, respectively.

In order to get the doping of UiO-66 MOF, whose structure is characterized by 12-connected Zr_6-cluster node and terephthalic acid as main linker, with the ***Ni-bisdpmCOOH*** units, we followed the procedure reported by Sun *et. al***Errore. Il segnalibro non è definito.** who succeeded for the first time to integrate the NiTCPP in the UiO-66 framework.

By considering the structural analogy of ***Ni-bisdpmCOOH*** with NiTCPP the doping of UiO-66 MOF with ***Ni-bisdpmCOOH*** complex may occur by the substitution of the 12-connected Zr_6-cluster node with the 2 connected ***Ni-bisdpmCOOH,*** in line with the integration of 4-connected NiTCPP already reported by Sun *et. al***Errore. Il segnalibro non è definito.** (see Figure 8).

Furthermore, this can be supported by the compatible length of the auxiliary linkers evaluated as the distance between the C atoms of two opposite carboxylic groups in relation to the maximum extension of the original 12-connected Zr6-cluster node evaluated to be *ca*. 20.8 Å. Such values correspond to 18.2 Å for ***Ni-bisdpmCOOMe,*** reasonable similar to that of ***Ni-bisdpmCOOH***, and to 18.4 Å in the case of NiTCPP.

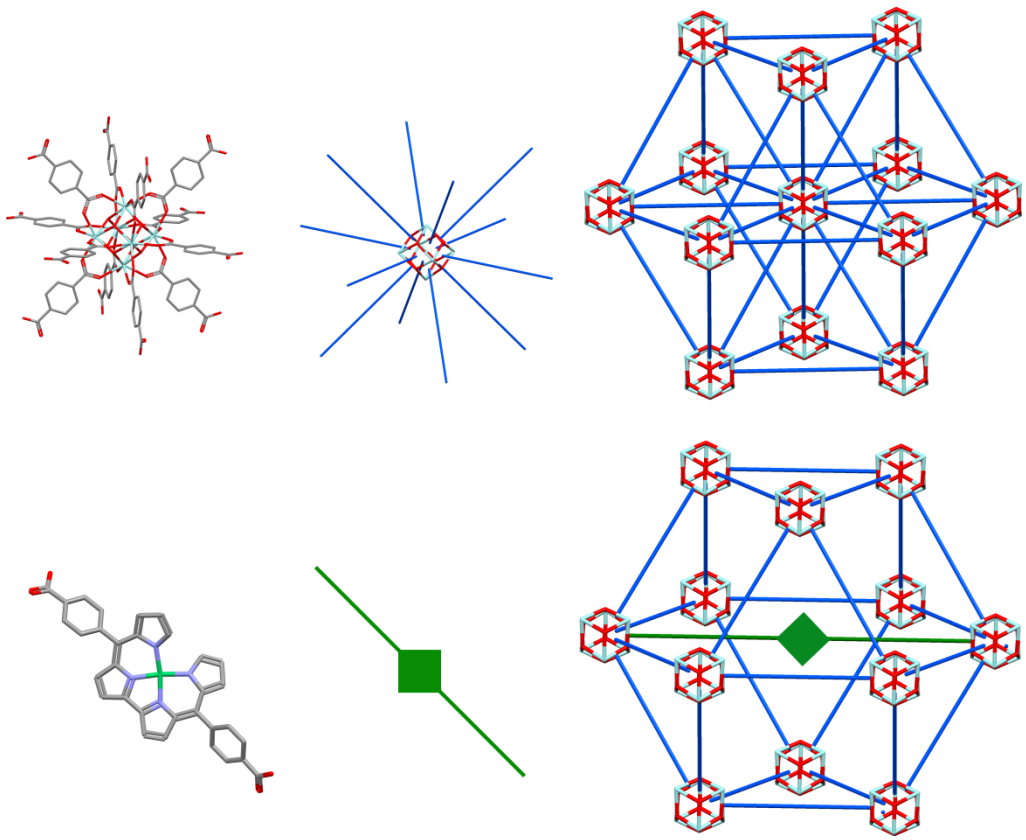

Figure 8 *– UiO-66 structure (top) and schematic illustration of its doping with* ***Ni-bisdpmCOOH*** *(bottom).*

The successful doping of UiO-66 MOF with ***Ni-bisdpmCOOH*** can be evidenced by the formation of a black coloured microcrystalline powder, characterized by a unique crystalline phase perfectly corresponding to that of the original UiO-66 framework, as shown by XRPD analysis reported in Figure 9.

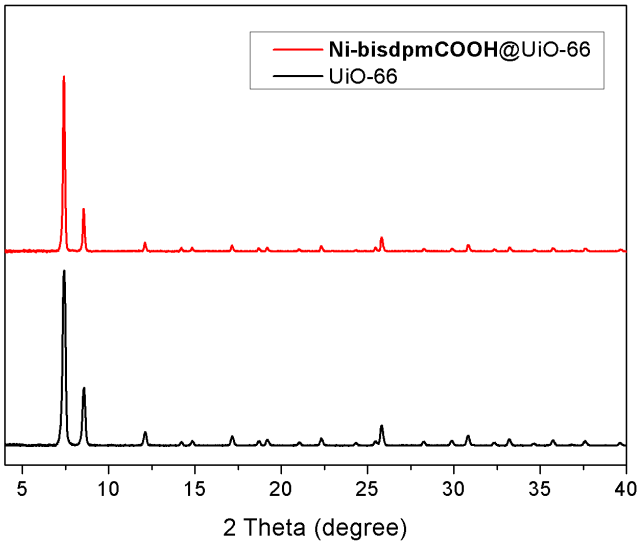

Figure 9 *– XRPD pattern for* ***Ni-bisdpmCOOH****@UiO-66 (top) and UiO-66 (bottom)*

To demonstrate the effective incorporation of ***Ni-bisdpmCOOH*** in the UiO-66 framework, and to rule out any clathration of the molecule inside the framework, control reactions were performed.

In particular, the use of complex ***Ni-bisdpmCOOMe*** as dopant linker resulted in a white crystalline material as the bare UiO-66 framework. This clearly demonstrates that the absence of free carboxylic acid coordinating groups prevent the incorporation of such linker into the MOF framework.

Similar results were attained by using as dopant the demetalated molecule ***bisdpmCOOH***, thus underlying the key role played by the coordinating Ni center to give the necessary structural rigidity to the molecule for being successfully incorporated as auxiliary linker.

A further proof of the effective doping comes from the similar UV-vis absorption properties shown by ***Ni-bisdpmCOOH*** and ***Ni-bisdpmCOOH***@UiO-66, as clearly evidenced by the corresponding diffuse reflectance spectra reported in Fig. 10, i.e. both displaying comparable main absorption peaks at *ca.* 450 and 500 nm, with a broad absorption above 550 nm.

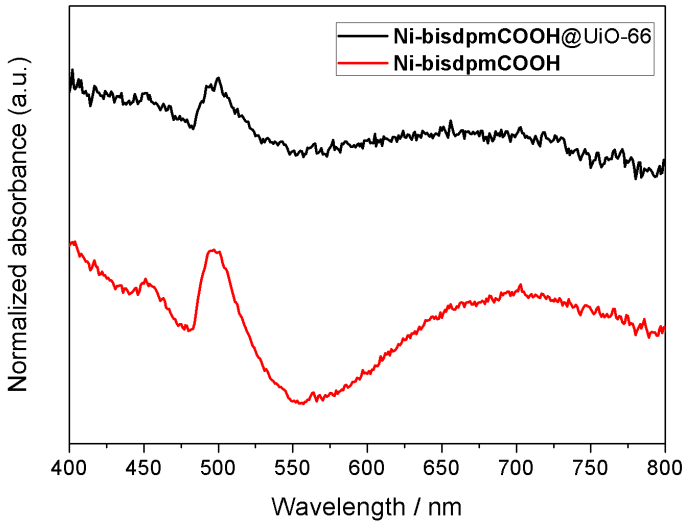

Figure 10 *– DRS spectra of* ***Ni-bisdpmCOOH*** *(bottom) and doped framework (top)*

The photoelectrochemical activation of this successfully prepared ***Ni-bisdpmCOOH***@UiO-66 MOF for solar into chemical energy conversion is currently under investigation.

4. Conclusions

In conclusion, we have fully characterized the photophysical and electrochemical properties of ***Ni-bisdpmCOOH*** as representative example of an intriguing class of bisdipyrrin complexes.

The effective ability of ***Ni-bisdpmCOOH*** to act as a rather good sensitizer of TiO_2-based photoanode, i.e. enabling photocurrent production up to 620 nm irradiation, has been demonstrated.

Furthermore, the successfully doping of the highly stable UiO-66 MOF with this promising visible light sensitizer represents a preliminary but necessary step for developing new multifunctional materials with photocatalytic applications.

---

[1] (a) Kowada, T.; Maeda, H.; Kikuchi, K., *Chem. Soc. Rev.*, **2015**, *44*, 4953; (b) Lu, H.; Mack, J.; Yang, Y.; Shen, Z., *Chem. Soc. Rev.*, **2014**, *43*, 4778; (c) Benstead, M.; Mehl, G. H.; Boyle, R. W., *Tetrahedron*, **2011**, *67*, 3573; (d) Loudet, A. Burgess, K., *Chem. Rev.*, **2007**, *107*, 4891.

[2] (a) Ikeda, C.; Ueda, S.; Nabeshima, T. *Chem. Commun.*, **2009**, 2544; (b) Sakamoto, N.; Ikeda, C.; Yamamura, M.; Nabeshima, T. *J. Am. Chem. Soc.*, **2011**, *133*, 4726; (c) Ishida, M.; Naruta, Y.; Tani, F. *Angew. Chem. Int. Ed.*, **2010**, *49*, 91; (d) S. A. Baudron, Dalton Trans., **2013**, *42*, 7498-7509.

[3] Hall, J. D.; McLean, T. M.; Smalley, S. J.; Waterland, M. R.; Telfer, S. G. *Dalton Trans.*, **2010**, *39*, 447.

[4] Liu, X.; Nan, H.; Sun, Q.; Zhang, Q.; Zhan, M.; Zou, L.; Xie, Z.; Li, X.; Lu, C.; Cheng, Y. *Dalton Trans.*, **2012**, *41*, 10199.

[5] Bronner, C.; Baudron, S. A.; Hosseini, M. W.; Strassert, C. A.; Guenet, A.; De Cola, L. *Dalton Trans.*, **2010**, *39*, 180.

[6] (a) Hanson, K.; Tamayo, A.; Diev, V. V.; Whited, M. T.; Djurovich, P. I.; Thompson, M. E. *Inorg. Chem.*, **2012**, *18*, 4041; .(b) Bronner, C.; Baudron, S. A.; Hosseini, M. W. *Inorg. Chem.*, **2010**, *49*, 8659; (c) Bronner, C.; Veiga, M.; Guenet, A.; Hosseini, M. W.; De Cola, L.; Strassert, C. A.; Baudron, S. A. *Chem.-Eur. J.*, **2012**, *18*, 4041.

[7] (a) Falk, H.; Neufingerl, F. *Monatsh. Chem.*, **1979**, *110*, 987; (b) Sazanovich, I. V.; Kirmaier, K.; Hindin, E.; Yu, L.; Bocian, D. F.; Lindsey, J. S.; Holten, D. *J. Am. Chem. Soc.*, **2004**, *126*, 2664; (c) Maeda, H.; Hashimoto, T.; Fujii, R.; Hasegawa, M. *J. Nanosci. Nanotechnol.*, **2009**, *9*, 240; (d) Lee, S.; Seok, C.-H.; Park, Y.; Lee, A.; Jung, D. H.; Choi, S.-H.; Park, *J. Mol. Cryst. Liq. Cryst.*, **2010**, *531*, 65; (e) Kusaka, S.; Sakamoto, R.; Kitagawa, M.; Okumura, M.; Nishihara, H. *Chem.-Asian J.*, **2012**, *7*, 907; (f) Sakamoto, R.; Kusaka, S.; Kitagawa, Y.; Kishida, M.; Hayashi, M.; Takara, Y.; Tsuchiya, M.; Kakinuma, J.; Takeda, T.; Hirata, K.; Ogino, T.; Kawahara, K.; Yagi, T.; Ikehira, S.; Nakamura, T.; Isomura, M.; Toyama, M.; Ichikawa, S.; Okumura, M.; Nishihara, H. *Dalton Trans.*, **2012**, *41*, 14035; (g) Yang, L.; Zhang, Y.; Yang, Q.; Chen, Q.; Ma, J. S. *Dyes Pigm.*, **2004**, *62*, 27; (h) Hashimoto, T.; Nishimura, T.; Lin, J. M.; Khim, D.; Maeda, H. *Chem.-Eur. J.*, **2010**, *16*, 11653.

[8] Orłowsk, R.; Gryko, D.; Gryko, D. T., *Chem. Rev.*, **2017**, *117*, 3102.

[9] Johnson, A. W.; Price, R., *J. Chem. Soc.*, **1960**, 1649.

[10] (a) Bröring, M.; Brandt, C. D.; Lex, J.; Humpf, H.-U.; Bley-Escrich, J.; Gisselbrecht, J.-P., *Eur. J. Inorg. Chem.*, **2001**, 2549; (b) Bröring, M.; Brandt, C. D.; Bley-Escrich, J.; Gisselbrecht, J.-P., *Eur. J. Inorg. Chem.*, **2002**, 910; (c) Baudron, S. A.; Ruffin, H.; Hosseini, M. W., *Chem. Commun.*, **2015**, *51*, 5906; (d) Baudron, S. A.; Hosseini, M. W., *Chem. Commun.*, **2016**, *52*, 13000.

[11] (a) Kong, J.; Li, Q.; Li, M.; Li, X.; Liang, X.; Zhu, W.; Ågren, H.; Xie, Y. *Dies and Pigments*, **2017**, *137*, 430; (b) Gill, H. S.; Finger, I.; Božidarević, I.; Szydlo , F.; Scott, M. J. *New J. Chem.*, **2005**, *29*, 68.
[12] Halper, S. R. and Cohen, S. M., *Inorg. Chem.* **2005**, *44*, 486.
[13] Artigau, M.; Bonnet, C.; Ladeira, S.; Hoffmann, P.; Vigroux, A. *CrystEngComm.*, **2011**, *13*, 7149.
[14] Due to solubility issues, the proton integration in the ^{1}H NMR spectrum is hampered.
[15] Brückner, C.; Zhang, Y.; Rettig, S. J.; Dolphin, D. *Inorg. Chim. Acta A*, **1997**, *263*, 279.
[16] Dozzi, M. V.; Marzorati, S.; Longhi, M.; Coduri, M.; Artiglia, L.; Selli, E Applied Catalysis B: Environmental, 2016, 186, 157.

[17] Kumar, B.; Llorente, M.; Froehlich, J.; Dang, T.; Sathrum, A.; Kubiak, C. P., *Annu. Rev. Phys. Chem.*, **2012**, *63*, 541.
[18] Imahori, H.; Hayashi, S.; Hayashi, H.; Oguro, A.; Eu, S.; Umeyama, T.; Matano, Y. *J. Phys. Chem. C*, **2009**, *113*, 18406.
[19] (a) Zhang, T.; Lin, W, *Chem. Soc. Rev.*, **2014**, *43*, 5982; (b) Silva, P.; Vilela, S. M. F.; Tome, J. P. C.; Almeida Paz, F. A., *Chem. Soc. Rev.*, **2015**, *44*, 6774; (c) Furukawa, H.; Müller, U.; Yaghi, O. M., *Angew. Chem. Int. Ed*., **2015**, *54*, 3417; (d) Deng, H.; Doonan, C. J.; Furukawa, H.; Ferrerira, R. B.; Towne, J.; Knobler, C. B.; Wang, B; Yaghi, O. M., *Science*, **2010**, *327*, 846.
[20] He, J.; Wang, J.; Chen, Y.; Zhang, J.; Duan, D.; Wang, Y.; Yan, Zhiying, Y. *Chem. Commun.*, **2014**, *50*, 7063.